Comment on “elastic-plastic deformation in ion-exchanged aluminosilicate glass by loading rate dependent nanoindentation”

Gwenole Trenvouez, Jean-Pierre Guin, V. Keryvin, Cédric Bernard

▶ **To cite this version:**

Gwenole Trenvouez, Jean-Pierre Guin, V. Keryvin, Cédric Bernard. Comment on “elastic-plastic deformation in ion-exchanged aluminosilicate glass by loading rate dependent nanoindentation”. Journal of Non-Crystalline Solids, 2020, 528, pp.119692. 10.1016/j.jnoncrysol.2019.119692 . hal-02357339

HAL Id: hal-02357339
https://hal.science/hal-02357339v1

Submitted on 21 Dec 2021

HAL is a multi-disciplinary open access archive for the deposit and dissemination of scientific research documents, whether they are published or not. The documents may come from teaching and research institutions in France or abroad, or from public or private research centers.

L’archive ouverte pluridisciplinaire **HAL**, est destinée au dépôt et à la diffusion de documents scientifiques de niveau recherche, publiés ou non, émanant des établissements d’enseignement et de recherche français ou étrangers, des laboratoires publics ou privés.

Distributed under a Creative Commons Attribution - NonCommercial 4.0 International License

Version of Record: https://www.sciencedirect.com/science/article/pii/S0022309319305630
Manuscript_c6439155529a1359ecbb6864179759f1

Comment on "Elastic-plastic deformation in ion-exchanged aluminosilicate glass by loading rate dependent nanoindentation"

G. Trenvouez[a], J.-P. Guin[a,*], V. Keryvin[b], C. Bernard[b]

[a] *Univ Rennes, CNRS, IPR (Institut de Physique de Rennes) - UMR 6251, F-35000 Rennes, France*
[b] *Univ Bretagne Sud,CNRS, iRDL - UMR 6207, F-56100 Lorient, France*

Abstract

As part of a recent study Li et al. [1] proposed as a proof of inhomogeneous shear flow at indentation site in oxide glasses the existence of both a nano pattern on the residual imprint as revealed by atomic force microscopy and numerous discrete events on the load displacement curve, called bursts. Both were reported to be loading rate dependent. Here, using the same experimental set up, we provide experimental evidence that discrete bursts existence and loading rate sensitivity can be attributed to the displacement sensor noise floor and to data sampling rate issues respectively. We also show the nano pattern present on the faces of the indentation imprint to be extremely repeatable, to not depend neither on glass composition nor on loading rate as it is the result of the stamping onto the glass surface of the indenter surface roughness generated by its machining process.

Keywords: Glass, Plastic deformation, Nanoindentation/AFM, Loading rate

1. Introduction

Evidences for the occurrence of plastic deformation in oxide glasses dates back 70 years ago [2], yet the atomistic mechanisms responsible for the incipient plasticity under sharp contact are hardly identified and known. Numerical modeling can provide interesting assumptions [3, 4, 5] which are extremely difficult to observe experimentally essentially because

*Corresponding author
Email addresses: gwenole.trenvouez@univ-rennes1.fr (G. Trenvouez), jean-pierre.guin@univ-rennes1.fr (J.-P. Guin), vincent.keryvin@univ-ubs.fr (V. Keryvin), cedric.bernard@univ-ubs.fr (C. Bernard)

© 2019 published by Elsevier. This manuscript is made available under the CC BY NC user license
https://creativecommons.org/licenses/by-nc/4.0/

of the length scale (atomic cluster) at stake. Nonetheless the understanding of such plastic mechanisms in glass are of paramount importance as their complete understanding may provide paths for strength improvement [6, 7] and trigger innovative applications of glass. Thus experimental observations at very low scale are a corner stone. Yet they must be free of artifact in order not to mislead the glass community. In their recent work on the elastic-plastic deformation in raw and ion-exchanged aluminosilicate glass studied by loading rate dependent nanoindentation X. Li and co worker [1] concluded that the patterns observed on the residual indentation imprint faces to be flow lines resulting from shear stress developing during the indentation process. They also reported that flow lines were more pronounced at low loading rates than at higher ones. Moreover, from the indentation load-displacement curves they observed that many discrete bursts of rapid displacement at almost constant load were occurring for the lowest values of the loading rate. Those bursts disappeared for the higher loading rates and were described to be related to instantaneous shear flow processes called serration in agreement with [8]. The discussion of the experimental results provided by the authors gives a rather elegant and satisfactory justification for their observations, nonetheless we do not agree with their conclusions. Therefore the purpose of this comment is to provide the community clear and factual elements that will undoubtedly lead to more rational and supported conclusions regarding both the observation of bursts called serrations on the loading curve as well as the presence of what was named flow lines on the faces of nanoindentation imprints.

To strengthen our approach and statements two aspects were considered: first the indentation tests were made with an identical experimental set up using very similar experimental conditions as the ones used by Li et al. [1] (see experimentation part for further details); second, we chose two different glass compositions which exhibit two different mechanical behaviors regarding indentation testing [9, 10, 11]. A normal glass (a typical window glass) which deforms mainly through shear flow (a volume conservative mechanism) like the reported aluminosilicate composition in [1] and an anomalous glass (pure silica glass) which exhibits a large contribution of a non volume conservative mechanism referred as the permanent densification mechanism [12, 13, 14, 15].

2. Materials and Methods

2.1. Materials and surface preparation:

A window floated glass from Saint Gobain company was selected for this study, the composition is referenced in [16], the air side was selected for nanoindentation testing before which a thermal annealing of the specimen at Tg (the glass transition temperature) for 1 hour was performed in order to prevent the results from the effect of both the post process residual stresses and the sodium depletion of the outmost layer due to the effect of storage humidity over time. The second tested glass was a pure silica glass sample (Spectrosil FQ 300) from Heraeus, with a low OH content <3 ppm. Prior testing the indented surface was polished with alumina then cerium oxide as a finishing step. The sample was subsequently annealed at Tg for 1 hour in order to obtain properties of the outmost layer as close as it can be from the bulk properties.

2.2. Nanoindentation tests:

We used the same nanoindenter apparatus as the one used by X. Li and coworkers [1], a Hysitron Nanotriboscope TI950 from Bruker equipped with a standard nanoindentation head and a modified Berkovich indenter (15 nm truncated length). Indentation tests were carried out after the system reached a thermal equilibrium (few hours after samples mounting) the maximum load was set to 8 mN for the most recent study, 10 mN for the oldest that were carried on in 2007 and 2008 with the exact same Berkovich indenter. Loading rates were varied from 80 $\mu N.s^{-1}$to 16 000 $\mu N.s^{-1}$with a holding time of 10 s applied at maximum load before a decrease of the load back to zero within 10 seconds (see fig.1). For each indentation test, data sampling rate was set to 200 Hz. Temperature and humidity level were measured while the experimentation were performed (25°C, 44%RH). 5 indentation tests were performed for each loading condition.

2.3. Atomic force microscope (AFM):

After nano indentation testing the topography of the residual indentation imprint was imaged by AFM with the tapping^{TM} mode. A dimension 3100 with a Nanoscope V electronic (Bruckers, santa Barbara, USA) equipped with ARROW-NCR-50 aluminum back coated

silicon probes (tip radius better than 10 nm, spring constant of 42 N/m range with a resonance frequency of 285 kHz) from Nanoworld was used for this purpose. Due to both a smaller tip radius and a sharper apical angle when compared to those of the indenter, the geometry of the residual indentation imprint is not altered by the AFM tip. The (X-Y-Z) axis of the AFM were calibrated with several grids: a 10 μm pitch of 200 nm deep squared holes and a 3 μm pitch of (23±1) nm deep engraved features (TGZ1 grating from NT-MDT) before capturing the topography of the surface. Imaging conditions was chosen so that the effect of thermal drift on the small speed scan axis was limited (thermal equilibrium of the system was reached). Furthermore, the size of the scanned area was large enough so that a sufficient area unaffected by the indentation process exists and may be used later on as a reference surface (ie., set to zero tilt and zero offset) for image post treatment. Usual imaging parameters set up was used, squared images, which size ranges from 3,5 to 5 μm were captured with a digital resolution ranging from 4 nm/pixel up to 10 nm/pixel at a scan frequency set between 1 and 2 Hz. As indentation on glass is highly repeatable, 3 to 5 imprints were imaged for each loading condition.

2.4. Image treatment:

All the following AFM images post-treatment were performed with Gwyddion software [17].

• General image preparation : Raw AFM 3D data set was post treated so that the surface unaffected by the indentation process surrounding the residual imprint was used as a reference surface. It was supposed by definition to be flat and not tilted. Thus on this selected area a plane levelling (correction of tilt and offset) as well as a row alignment, which corrects slight differences of offset and tilt between the fast scan axis profiles were applied.

• Enhancing the contrast by Laplacian of a Gaussian filtering (LoG): Unfortunately the nano pattern of interest, which is present on the faces of the indentation imprint, is hardly observable on the topography image (fig. 2) because of the high vertical range of the indentation imprint topography when compared to the local roughness of the nano pattern (about 2 orders of magnitude difference). Enhancing the contrast of the digital image by

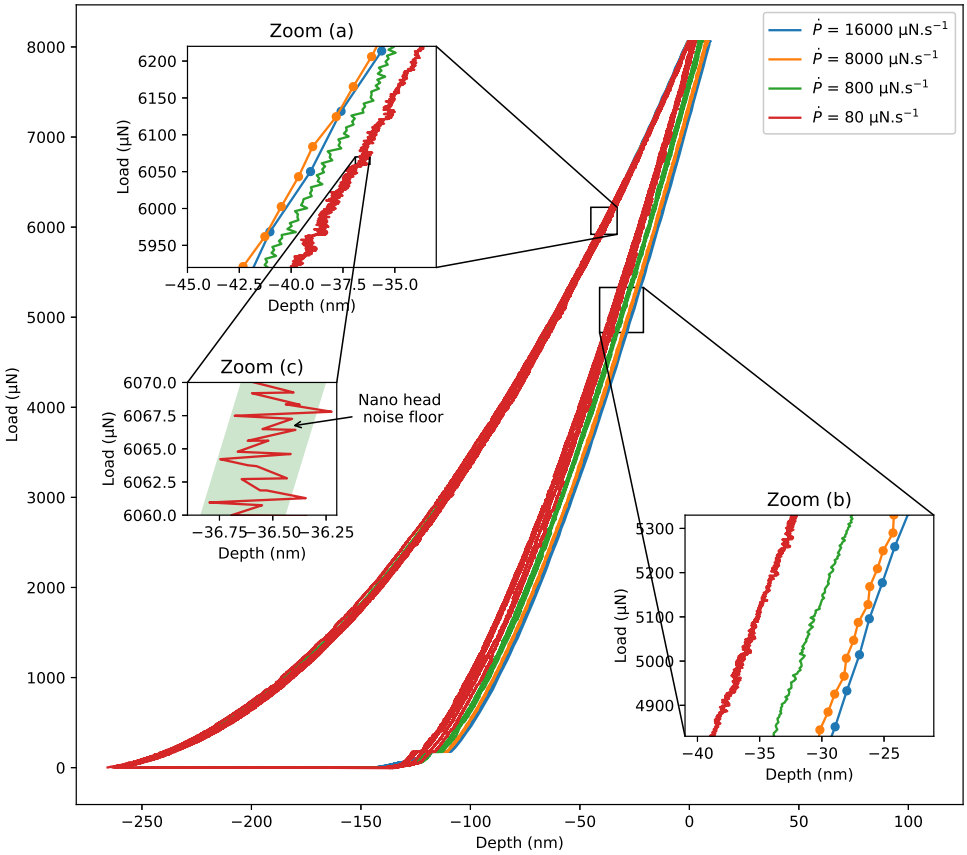

Figure 1: Berkovich indentation load-displacement curves made on window glass for various loading rates (80, 800, 8000, 16000 µN.s^{-1}with a data sampling rate of 200 Hz. Specific zones of interest have been zoomed in : left, zoom (a) on the loading portion, right, zoom (b) on the unloading portion. All the curves were re-positioned so that the penetration depth is the same at P_{max}. The greened area on zoom(c) represents the ± 0.2 nm RMS noise floor of the displacement sensor.

applying a Laplacian of a Gaussian (LoG) filter to the topographic image (see for instance [18] for deeper information regarding this filter) provides a convenient way for observing this nano scaled pattern more easily (see figures 2 and 3).

• Accessing the nano scaled roughness of an indentation imprint face: An other interesting information to extract would be the very local roughness of this pattern for comparison purposes between indentation conditions. However, the geometry of a full indentation imprint is quite complex. Therefore we chose to select one face out of the 3 faces of an indentation imprint (for instance face 2, see fig. 3) by masking the rest of the image (fig.4). We took care so that the selected face (the unmasked region) covered the exact same spatial

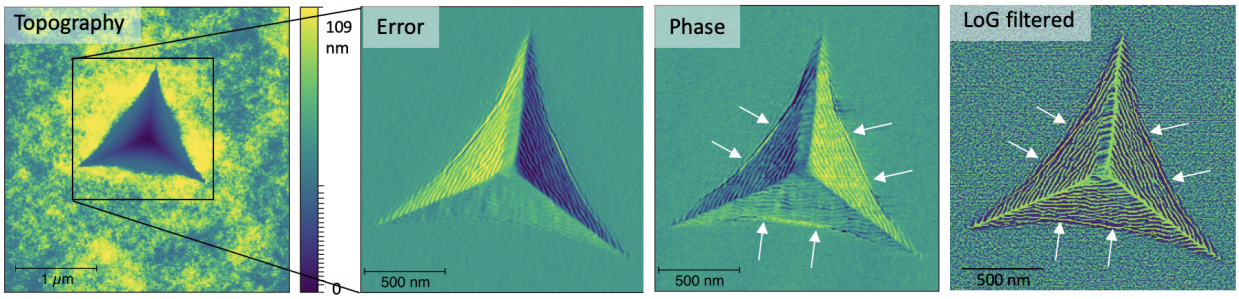

Figure 2: 8 mN Berkovich indentation imprint on silica glass ($\dot{P} = 800$ µN.s^{-1}) imaged by AFM: from left to right the topography, the Error contrast signal, the Phase contrast signal and the LoG filtered image are shown with the same in plane scaling. White arrows illustrate crack running along each face of the indentation imprint (phase and LoG contrasts).

zone (at better than ± 10 nm) for each indentation imprint reported in figure 4 (h). Then the local curvature and mis orientation was suppressed by a 2nd order polynomial form along the x and the y directions without affecting the nano pattern roughness (long wave length action when compared to the nm scale characteristic length of the nano pattern). More subtle ways such has windowed FFT filtering may also be used but we found the 2nd order polynomial form simple to use and its effect on the geometry easy to understand. The result of such a filtering is illustrated in figure 4.

3. Existence of serration on load displacement curves

In their work X. Li [1] and co workers reported the existence of serrations on load-displacement curves during the loading phase under slow loading rates conditions (100 to 2000 µN.s^{-1}) and their vanishing for the fastest loading rates (10000 and 20000 µN.s^{-1}). The Authors suggested the existence of a link between loading rate and the frequency of serration phenomenon. However, one aspect that X. Li et al. have not considered in their study is the possible effect of the data sampling rate on the load-displacement curves aspect. The value they used in their study is not mentioned, nevertheless a careful look at the figure 10 of their work suggests they used a 200 Hz value, which is the value we chose for our tests (fig. 1).

The indentation load-displacement curves obtained both on silica and SLS glasses (fig. 1 reports only the SLS glass case) exhibit, between low loading rates (80 and 800 µN.s^{-1})

and high loading rates (8000 and 16000 $\mu N.s^{-1}$), the same contrast as the one reported by X. Li et al. for an alumino silicate glass. Discrete burst events at almost constant load (called serrated events) are observed on the loading curve of the smallest loading rate (80 $\mu N.s^{-1}$, they are still visible at 800 $\mu N.s^{-1}$but disappear for higher loading rates (8000 and 16000 $\mu N.s^{-1}$) see Fig. 1 : Zoom (a). More intriguing is that the same observations are made for the unloading part of our load-displacement curve (figure 1 : Zoom (b)) and no statistical differences could be detected between the loading and the unloading portions of the curve (figure S3 [19]) while from the literature it is purely elastic (see for instance [20, 21]). Therefor no plastic events should occur during the unloading portion and thus no burst events should be observed if they were related to plasticity[1]. From this observation, one might consider the fact that those discrete burst events are not related to the material's behavior but rather to indentation apparatus and set up. Following up on this trail two parameters of importance must be considered: firstly the data sampling rate at which data points are collected over time during the indentation test and secondly the RMS noise of the vertical (z) sensors (the load sensor effect is negligible as its noise floor to applied load ratio is lower than 10^{-3}). First, the disappearance of the discrete bursts at high loading rates is illustrated by both figures 1 : Zooms (a and b) for which the data points collected at a rate of 200 Hz are drawn as filed circles only for the two highest loading rates. It is clear that the lack of data points acts as a low pass filter and leads to the progressive flattening of the indentation curves as the loading rate increases, thus to the disappearance of the discrete events. Furthermore, those observations are well reproduced when comparing indentation curves made at different loading rates (80 and 8000 $\mu N.s^{-1}$) with the same density of measurements per μN N (see figure S1 and S2 in [19]). Second, the RMS noise floor of the Z displacement sensor is equal to $\pm$ 0.2 nm according to Hysitron. The greened area on figure 1 : Zoom (c) represents the RMS noise floor of the system for a portion of the lowest loading rate load-displacement curve. In other words and according to a Normal law,

[1]Unfortunately Li et al. [1] did not provide the unloading part of their load-displacement curves with enough resolution. Nonetheless the present observation and remark apply also to the work by Dey et al. [22] cited in [1] who observed "pop-in" phenomenon for SLS glass on indentation load-displacement curves, which they related to the formation of deformation bands.

any discrete burst events to be detected with a 68.2% (95%) confidence must be outside the ± 0.2 nm (± 0.4 nm) greened bandeau. As a conclusion for this part, we found the reported discrete burst events to result mainly from the z vertical sensor noise provided a large enough data sampling rate is used. To detect this kind of discrete events with a 95% confidence, the amplitude of their signature would have to be larger than 0.4 nm.

4. Origin of the nano patterns

As mentioned earlier we intend to propose another explanation for the features or patterns observed by X. Li et al.[1]. In the present study we used the exact same indenter to perform all the indentation tests, even those that were performed seven to eight years ago. During AFM imaging of the residual imprint, the topography, the error signal and the phase contrast were recorded (fig. 2). First of all, as Li et al [1] we also do observe nano patterns on the faces of residual imprints for silica or SLS glass. This is observable both for the error contrast as well as for the phase contrast. The former is a derivative of the topography along the fast scan axis thus making it easier to observe tiny local slope changes while the later is linked to dissipative phenomena during contact between the tip and the surface while the tip is oscillating. These dissipative phenomenon may arise for different reasons such as local variations of adhesion conditions or any reason that will affect the contact surface (local elasticity variation, local roughness). In our case the local roughness should be the main reason for such a pattern to be observed as it is supported by the error signal and the LoG contrast.

The zoomed-in areas of figure 2 (i.e. error, phase and LoG signals) do represent the same indentation imprint for which the three edges of the Berkovich indenter are easily recognized. One of the edges present a peculiar pattern which provides help regarding the orientation of the imprint. All three faces do present the same kind of nano pattern which is made of alternation of depressions and hills that do form sinuous valleys or hills lines parallel to each others and to the base of the triangle formed by the considered face. The period between two depressions or hills is (24.6 ± 3.5) nm and the amplitude (vertical distance between two consecutive pic and valley) lies between 0.4 and 4.8 nm having a mean value of about

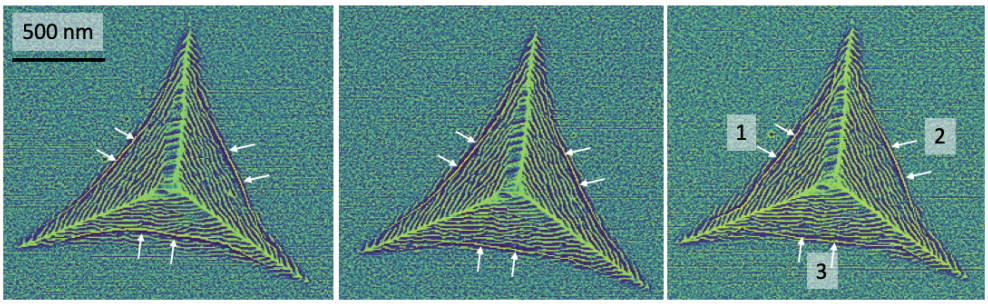

Figure 3: LoG filtered topographic images of three different Berkovich indentation imprints made at P_{max} = 8 mN, $\dot{P}$ = 800 µN.s^{-1}on the silica glass sample. White arrows illustrate differences in the pattern resulting from the presence of cracks. Numbers 1, 2, 3 on the right hand figure are the numbers given to the three different faces of the residual imprint.

1.9 nm.

4.1. Repeatability of the pattern

Three indentation imprints 10 µm apart from each others were made using the same experimental conditions (Berkovich indenter, P_{max} = 8 mN, $\dot{P}$ = 800 µN.s^{-1}) on the same silica glass sample. The residual imprints were retrieved right after for AFM imaging of their topography. A LoG filter was subsequently applied to the topography in order to enhance the contrast of its local variations (fig. 3). One of the 3 edges of the indenter (between face 1 and 2) presents a peculiar pattern that certainly results from an uneven wear during scratch testing. With this indenter tip, this pattern is extremely repeatable from one imprint to the other and further provides some help for recognizing and comparing the same indentation face from one imprint to the others. In the three-sided indentation imprint, regardless of the face number i considered (i=1, 2, 3), the pattern formed by the alternations of green and dark blue lines is exactly the same from one face i to another face i at the exception of the lines highlighted by two white arrows. The later illustrate lines mostly parallel to the base of the considered face. Those lines are the signature of cracks that developed during the indentation process. The random nature of both the fracture phenomenon and the glass structure lead to slight differences in shape and position between the same face i of the 3 different indentation imprints reported in figure 3. Therefore those nano patterns are highly reproducible from one indentation to another. It is also of interest to compare

directly the nano-scaled topography from which originates the LoG filter contrast discussed above. In order to do so the procedure described in the third point of the image treatment section of part 2 was applied to each AFM image. Resulting topographies of the number 2 faces of indentation imprints are reported in figure 4 for different indentation conditions and glasses. Figure 4 (a-c) illustrates the nano-scaled topography of the number 2 faces of the indentation imprints presented in figure 3. Because the nano-scaled patterns look rather identical and for the sake of readability, white arrows pointing at 4 selected features traceable from one indentation imprint to the other were added. Moreover AFM images of 10 mN Berkovich indentation imprints that were done 8 years apart from the recent ones with the same indenter (fig. 4 (e)) exhibit a nano-scaled topography very similar to the one previously discussed. Slight differences are mostly due to variations of spatial resolution coming from both a different finite size of the AFM probe tip used for imaging and from differences in numerical spatial resolution (i.e. nm/pixel value). As a conclusion of this part the nanoscale roughness of an indentation face made on a silica glass is highly repeatable down to the nanometer scale from an indentation to another one and even throughout the years.

4.2. Effect of the loading rate

For amorphous silica glass the effect of the loading rate (from 80 to 16 000 $\mu N.s^{-1}$) upon the nano scaled roughness present on each indentation imprint face and more specifically on the number 2 face was investigated. Although indentation imprint reported in (figure 4 (d)) was made at a loading rate ten times faster (i.e. 8000 $\mu N.s^{-1}$) than imprints a to c (figure 4 (a-c)), nano scaled patterns observable on the selected face number 2 look rather similar. The same observations were made whatever the considered loading rate. Therefore it can be safely concluded that the loading rate, within the studied range, has no effect on the nano-scaled topography observed on the faces of a nano indentation imprint.

4.3. Effect of glass composition

To study the effect of glass composition on the nano pattern, indentations made on SLS glass were also imaged by AFM. Contrarily to silica glass, SLS glass is a normal glass which

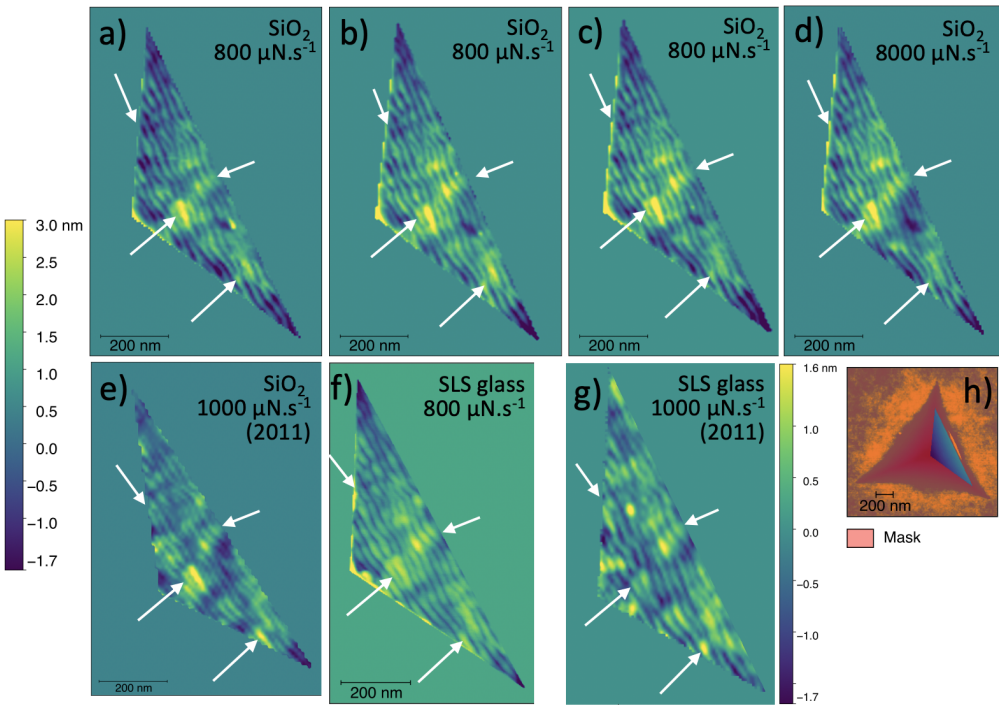

Figure 4: Topography images of the selected face numbered 2 (h) for different residual indentation imprints produced by the same indenter throughout experimental conditions and years. Curvature of the face was corrected by a 2^{nd} order X and Y polynomial form leaving only the nanometer scale roughness visible. a, b, c) SiO_2 8 mN maximum load at $\dot{P} = 800$ µN.s^{-1}; d) SiO_2 8 mN maximum load at $\dot{P} = 8000$ µN.s^{-1}; e) SiO_2 10 mN maximum load at $\dot{P} = 1000$ µN.s^{-1}in 2011 ; f) SLS glass at $P_{max} = 8$ mN, $\dot{P} = 800$ µN.s^{-1}; g) SLS glass at $P_{max} = 10$ mN, $\dot{P} = 1000$ µN.s^{-1}; h) illustration of the selected face out of three for each indentation imprint, the reddish area is the mask used to exclude the rest of the data from numerical data treatment. z scale reported on the left inside is the same for every image except for: g), given on the right side and h), not provided. White arrows are drawn in order to help the reader to locate the same features on the different images of this set.

is described as being more prone to shear flow when compare to anomalous glass like silica. The indentation behavior of the SLS glass should be similar to the one of the aluminosilicate glass used in [1] as they are both normal glasses. Moreover a maximum densification ratio of SLS glass about 6% [23, 24] is expected while for the elastic properties of aluminosilicate glasses this ratio should lie between 5 to 7% according to [25]. As silica and SLS glasses exhibit very different indentation behavior more specifically regarding their permanent deformation mechanisms, we should expect differences in the nano patterns present on the indentation faces. For SLS glass the nano topography of face 2 is reported for two slightly different experimental conditions (Fig. 4 (f and g)), the maximum load (8 mN and 10

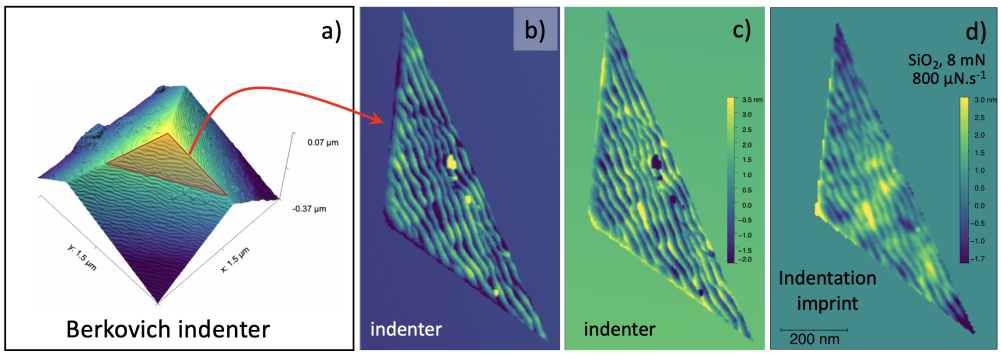

Figure 5: a) AFM image of the 3D topography of the Berkovich indenter used in this study. In red is a selected area on face number 2 of the indenter, b) topography of the reddish selected zone in a); the locally bright yellow zones are dusts; c) same image as in b) but presented with negative contrast for direct comparison with d); d) AFM image of the face number 2 selected in a Berkovich indentation imprint made on silica (load is 8 mN, loading rate 800 $\mu N.s^{-1}$). Image a, b and c were obtained with a Dimension Icon system from Bruker in the peak force tapping mode (see supplemental materials for more details [19]).

mN) was reached within 10 s but the two indentation imprints where made 7 years apart from each other. Similarly to silica glass, the small features of the surface topography are highly reproducible from one indentation to the other, differences rising mostly from the aforementioned reasons. For instance a higher digital lateral resolution (more pixel per nm) was used for figure 4 (f) but the AFM tip was slightly broader. More interesting is the fact that features highlighted by white arrows for silica (fig. 4 (a-e)) are also observed for SLS glass. It can be concluded that the features of the nano scaled pattern encountered on the surface of the face of nano indentation imprints are almost not affected by the anomalous or normal nature of the glass behavior. Furthermore for both silica and SLS glasses, indentation imprints made years apart with the same indenter exhibit the same nano scaled pattern.

As a conclusion for this part the nano scaled pattern observed on the indentation face is highly reproducible from one indentation to the other. It is affected neither by the indentation site, nor by the loading rate, nor even by the glass composition (normal to anomalous indentation behavior). Considering the amorphous nature of glass as well as the subsequent random spatial distribution of permanent deformation mechanisms onset (densification and shear flow) under the indenter should those nano patterns were flow lines (i.e. incipient plastic mechanisms) they would have reflected this random nature. Thus, in a logical way

differences are to be expected in this nano pattern either from one indentation imprint to the other when made on a same glass or above all from indentation imprints made on a normal and anomalous glass. The only explanation for such a reproducibility of this nano pattern lies in the transfer of pre-existing nano features from the indenter to the glass surface by a stamping process during the indentation test. For instance, Gadelrab and Chiesa [26] show the existence of such a nano roughness pattern present on the indenter faces that is similar in its nature to the nano pattern observed in our case on the imprint faces. They attributed the origin of this nano roughness to the manufacturing process [27, 28] of the diamond nanoindenter. Therefore the same pattern is embossed to the indented surface, indentation test after indentation test, year after year, providing wear does not alter it. Ideally, to avoid any doubts regarding this statement, one would like to observe the same nano pattern (one being the negative of the other) on both the indenter and the indentation imprint. The result of such an experiment is reported in Fig. 5 where the same nanometer scaled pattern (bumps, depressions, wavy lines, forks) can be observed on the topography image of both the indenter (fig 5c) and the imprint (fig 5d) made on silica glass with this same indenter. Glass reveals itself to be able to capture, with a great accuracy, by a room temperature embossing process the nanoscaled roughness of a diamond tool. The embossed nano pattern does not seem to be very sensitive to the normal or anomalous nature of the glass whereas the shape of the indentation imprint is [11]. A deeper and more specific study would be needed to strengthen this statement.

5. Conclusions

In this work we commented on the work done by X. Li et al [1], which proposed that nano patterns observed on the faces of residual indentation imprints of an alumino silicate glass are flow lines produced by shear displacements. The authors also linked those nano patterns to discrete events of rapid displacement at almost constant load, "pop-ins",observed on the indentation load vs.displacement curve. Furthermore they evidenced the impact of the loading rate on both observations: a disappearance of the former at high loading rates and a decrease of the number of flow lines with increasing loading rate. By using the same

experimental conditions and apparatus on so called normal (SLS glass) and anomalous (silica glass) glasses it is shown that:

• The discrete bursts observed for low loading rates on the load-displacement indentation curves result from the displacement sensor noise floor and contain no detectable material's behavior information. Their disappearance at high loading rates finds its explanation in a lack of data points because of an insufficient data sampling rate.

• Nano corrugations observed on the indentation imprint faces do not constitute a proof for the expression of incipient plasticity mechanisms like shear flow lines as mentioned by Li et al [1] but rather the trace of the existing nano roughness of the indenter faces that was stamped onto the glass surface (through a plastic deformation process) during indentation testing. The later provides a strong evidence regarding the fact that nano scaled and relatively complex patterns can be permanently transferred onto glass surfaces in a repeatable way. This nano pattern could be further used for a better estimation of the true contact area under maximum load [29].

• The pattern in the indentation imprint defined by the nano corrugations is neither loading rate dependant nor it is glass composition dependent. It is rather the finger print of the indenter as it was shown experimentally.

• Hence the present study invalidates the fact that serrations of the indentation load-displacement curve are closely related to the flow lines (nano corrugations) in the nanoindentation imprint. As a direct consequence, both arguments cannot be used to discuss the indentation behavior and its loading rate dependence of raw an ion exchanged aluminosilicate glasses.

6. Conflicts of interest

We declare no conflict of interest.

7. Acknowledgement

This work is supported: by the French Ministry of Higher Education for the PhD funding of G. Trenvouez; the European Union (ERDF), the ministry for Higher education, the Brit-

tany region and Rennes Métropole through the CPER Projects PRIN2TAN and GLASS. We would like to thank M. Nivard for her helpful advice regarding indentation experimentation and H. Orain for sample's preparation.

References

[1] X. Li, L. Jiang, J. Li, I. Mohagheghian, J. P. Dear, L. Li, Y. Yan, Elastic-plastic deformation in ion-exchanged aluminosilicate glass by loading rate dependent nanoindentation, Journal of Non-Crystalline Solids 491 (2018) 79–88.

[2] E. W. Taylor, Plastic deformation of optical glass, Nature 163 (1949) 323.

[3] B. Mantisi, G. Kermouche, E. Barthel, A. Tanguy, Impact of pressure on plastic yield in amorphous solids with open structure, Physical Review E 93 (2016) 033001.

[4] G. Molnár, . Ganster, A. Tanguy, Effect of composition and pressure on the shear strength of sodium silicate glasses: An atomic scale simulation study, Physical Review E 95 (2017) 043001.

[5] Z. Budrikis, D. F. Castellanos, S. Sandfeld, M. Zaiser, S. Zapperi, Universal features of amorphous plasticity, Nature communications 8 (2017) 15928.

[6] K. Januchta, M. M. Smedskjaer, Indentation deformation in oxide glasses: Quantification, structural changes, and relation to cracking, Journal of Non-Crystalline Solids: X 1 (2019) 100007.

[7] L. Wondraczek, J. C. Mauro, J. Eckert, U. Kühn, J. Horbach, J. Deubener, T. Rouxel, Towards ultrastrong glasses, Advanced Materials 23 (2011) 4578–4586.

[8] A. Dey, R. Chakraborty, A. K. Mukhopadhyay, Nanoindentation of soda lime–silica glass: effect of loading rate, International Journal of Applied Glass Science 2 (2011) 144–155.

[9] F. M. Ernsberger, Role of densification in deformation of glasses under point loading, Journal of the American Ceramic Society 51 (1968) 545–547.

[10] A. Arora, D. B. Marshall, B. R. Lawn, M. V. Swain, Indentation deformation/fracture of normal and anomalous glasses, Journal of Non-Crystalline Solids 31 (1979) 415–428.

[11] T. Rouxel, H. Ji, J. P. Guin, F. Augereau, B. Rufflé, Indentation deformation mechanism in glass: densification versus shear flow, Journal of applied physics 107 (2010) 094903.

[12] P. W. Bridgman, I. Šimon, Effects of very high pressures on glass, Journal of applied physics 24 (1953) 405–413.

[13] J. D. Mackenzie, High-pressure effects on oxide glasses: I, densification in rigid state, Journal of the American Ceramic Society 46 (1963) 461–470.

[14] V. Keryvin, J.-X. Meng, S. Gicquel, J.-P. Guin, L. Charleux, J.-C. Sanglebœuf, P. Pilvin, T. Rouxel, G. L. Quilliec, Constitutive modeling of the densification process in silica glass under hydrostatic compression, Acta Materialia 62 (2014) 250 – 257. doi:https://doi.org/10.1016/j.actamat.2013.07.067.

[15] V. Keryvin, L. Charleux, R. Hin, J.-P. Guin, J.-C. Sanglebœuf, Mechanical behaviour of fully densified silica glass under vickers indentation, Acta Materialia 129 (2017) 492–499.

[16] Y.-F. Niu, K. Han, J.-P. Guin, Locally enhanced dissolution rate as a probe for nanocontact-induced densification in oxide glasses, Langmuir 28 (2012) 10733–10740.

[17] D. Nečas, P. Klapetek, Gwyddion: an open-source software for SPM data analysis, Central European Journal of Physics 10 (2012) 181–188. doi:10.2478/s11534-011-0096-2.

[18] F. Neycenssac, Contrast enhancement using the laplacian-of-a-gaussian filter, CVGIP: Graphical Models and Image Processing 55 (1993) 447–463.

[19] G. Trenvouez, J.-P. Guin, V. Keryvin, C. Bernard, Comment on "elastic-plastic deformation in ion-exchanged aluminosilicate glass by loading rate dependent nanoindentation", supplementary material, Journal of Non-Crystalline Solids (2019).

[20] W. C. Oliver, G. M. Pharr, An improved technique for determining hardness and elastic modulus using load and displacement sensing indentation experiments, Journal of materials research 7 (1992) 1564–1583.

[21] M. F. Doerner, W. D. Nix, A method for interpreting the data from depth-sensing indentation instruments, Journal of Materials Research 1 (1986) 601–609. doi:10.1557/JMR.1986.0601.
[22] A. Dey, R. Chakraborty, A. K. Mukhopadhyay, Enhancement in nanohardness of soda–lime–silica glass, Journal of non-crystalline solids 357 (2011) 2934–2940.
[23] H. Ji, V. Keryvin, T. Rouxel, T. Hammouda, Densification of window glass under very high pressure and its relevance to vickers indentation, Scripta Materialia 55 (2006) 1159–1162.
[24] A. Perriot, E. Barthel, G. Kermouche, G. Querel, D. Vandembroucq, On the plastic deformation of soda-lime glass–a cr3+ luminescence study of densification, Philosophical Magazine 91 (2011) 1245–1255.
[25] T. Rouxel, H. Ji, T. Hammouda, A. Moréac, Poisson's ratio and the densification of glass under high pressure, Physical review letters 100 (2008) 225501.
[26] K. R. Gadelrab, M. Chiesa, Numerically assisted nanoindentation analysis, Materials Science and Engineering: A 560 (2013) 267–272.
[27] W. J. Zong, D. Li, T. Sun, K. Cheng, Y. C. Liang, The ultimate sharpness of single-crystal diamond cutting tools—part ii: A novel efficient lapping process, International Journal of Machine Tools and Manufacture 47 (2007) 864–871.
[28] T. Schuelke, T. A. Grotjohn, Diamond polishing, Diamond and Related Materials 32 (2013) 17–26.
[29] L. Charleux, V. Keryvin, M. Nivard, J.-P. Guin, J.-C. Sangleboeuf, Y. Yokoyama, A method for measuring the contact area in instrumented indentation testing by tip scanning probe microscopy imaging, Acta Materialia 70 (2014) 249 – 258. doi:https://doi.org/10.1016/j.actamat.2014.02.036.